



Study on the Influence of Tunnel Excavation Blasting on the Safety of Accumulation Slope at the Entrance

Feng Huang^{1a}, Siyuan Li^{1*}, Shunhang Xue^{1b}, Yonghao Yang^{1c}, Shuangjiang Wu^{2d}

¹State Key Laboratory of Mountain Bridge and Tunnel Engineering, School of Civil Engineering, Chongqing Jiaotong University, Chongqing, China

²Chongqing Communications Construction (Group) Company Limited, Chongqing, China,

^a543745152@qq.com, ^{*}1611772134@qq.com

^b2245452743@qq.com, ^c934929989@qq.com

^d1355877682@qq.com

ABSTRACT. During the tunnel blasting, with the accumulation of blast damage in the accumulation layer, accidents such as slope landslide of the accumulation layer and tunnel collapse quickly occur. Based on the Qiaopingshan tunnel project in Chongqing, the stability of the accumulation slope under different blasting loads and the variation law of its velocity field, displacement field and force chain distribution between particles in the accumulation layer are studied by using FLAC3D-PFC3D coupling analysis method. And a new method is proposed to solve the safety factor of the slope of the accumulation layer coupled with the discrete element and the finite element, that is, the strength of the physical and mechanical parameters between the particles of the accumulation layer is reduced, and the ratio of the inter-particle tension and the cohesive force chain is used as the evaluation standard to solve the safety factor of the slope.

KEYWORDS: blasting vibration; continuous-discontinuous coupling; accumulation layer slope

1 INTRODUCTION

In the southwest mountainous area of China, the slope of the mountain tunnel portal mostly exists in the form of a loose accumulation body, which is loose and sensitive to explosion stress waves. When the tunnel is blasted into the hole, with the accumulation of explosion damage inside the accumulation layer, accidents such as slope landslide and tunnel collapse are prone to occur.

Researchers at home and abroad have carried out a lot of research work on the accumulation. [1] analysed and studied the strength parameters of loose deposits through indoor direct shear test and in-situ direct shear test. [2] conducted large-scale cyclic simple shear tests and post-cyclic monotonic simple shear tests on gravelly soils with different gravel contents (GC) and loading conditions. [3] used the discrete

element method (DEM) to numerically study the difference in mesoscale characteristics of SRM models considering irregular shapes and proportions.

Aiming at the dynamic response of slope under blasting load, [4] clarified the cumulative damage evolution law of microcrystalline limestone under cyclic blasting load and established an improved nonlinear cumulative damage evolution model based on the number of explosions. [5] studied the dynamic response characteristics and failure mechanism of coal slope with weak interlayer under blasting load, analysed the influence of dynamic load with different frequencies on the dynamic response of slope, and determined the natural frequency of slope. [6] studied the mechanism and characteristics of surrounding rock vibration induced by air shock wave overpressure in tunnel blasting excavation, and concluded that when the air shock wave overpressure of small section tunnel blasting is large, the surrounding rock will be induced to vibrate with high vibration speed, long duration, and slow attenuation. [7] obtained that the main forms of slope deformation under dynamic load are deep rotation and translational sliding displacement by conducting large-scale shaking table model tests.

Numerical simulation can be used to analyse the stability and failure mechanism of slope under blasting more simply and systematically. [8] used LS-DYNA software to establish an equal-scale numerical model of a mountainside tunnel and studied the blasting vibration characteristics of a mountainside tunnel from three aspects: blasting parameters, slope characteristics and slope-tunnel geometric conditions. [9] used Midas numerical software to analyse the stability of the slope under blasting vibration conditions. [10] used ANSYS/LS-DYNA program to establish a three-dimensional (3D) slope model, analysed the influence of slope effect and whiplash effect on blasting vibration velocity in slope area and explored the variation law of blasting vibration velocity under different elevation conditions. Hamid Reza Mohammadi Azizabadi [11] used the general discrete element program (UDEC) to predict the particle velocity time history of blasting vibration in the mine wall, and the simulated particle velocity time history is in good agreement with the measured production blasting time history.

FLAC3D-PFC3D coupling analysis method is used to establish a three-dimensional coupled numerical model of the accumulation slope at the tunnel entrance, the stability of the accumulation slope under blasting action and the variation law of its internal velocity field, displacement field and force chain distribution among particles in the accumulation layer are studied. The research results can provide a theoretical basis for the design and construction of tunnel entrances.

2 PROJECT PROFILE

Qiaopingshan Tunnel Project is located at the northeastern end of Fangdoushan, Wanzhou District, Chongqing, with a total length of 2469m. The topography of the tunnel exit section is a reverse slope with a gradient of about 15 ~ 25, and the slope is a residual and landslide slope formed by natural accumulation. The slope of the tunnel entrance is located in the Quaternary slope collapse residual layer, which mainly in-

cludes silty clay and gravel soil. Silty clay is composed of fine sand and breccia, which are mainly distributed on the surface of the accumulation layer and the interface between soil and rock of the slope; Gravel soil is mainly composed of sandstone and mudstone, showing obvious angular shape, and the thickness of accumulation slope is about 5m. The surrounding rock of the tunnel entrance is mainly Grade IV surrounding rock, and the porosity of the accumulation layer is about 0.24. The overall discreteness of the slope of the accumulation layer at the entrance of the tunnel is large, the rock mass structure is loose and broken, and the bearing capacity of the surrounding rock is low. Under the action of tunnel excavation and blasting, the slope is easy to lose stability, which seriously threatens the safety of tunnel construction.

3 NUMERICAL SIMULATIONS

3.1 Computation module

According to the three-dimensional calculation model of tunnel entrance slope, the bedrock with good continuity is simulated by finite difference software FLAC3D, and the accumulation layer with large discreteness is simulated by discrete element software PFC3D. Then, the PFC model is embedded into the FLAC model, and the FLAC3D-PFC3D coupled numerical simulation information exchange channel is established. Based on the SocketI/O interface, the coupling calculation of the two algorithms is carried out. In each calculation step, the node velocity at the boundary of the FLAC model grid is transmitted to the particles in contact with the PFC model through the coupling wall, and the reaction force on the particles is transmitted to the boundary grid of the FLAC model through coupling. According to the mutual displacement relationship between the two models, the coordinates of the accumulation layer model are updated, and finally, the coordinates, velocity and force of the tunnel entrance slope [12] are updated (as shown in Figure 1). The FLAC3D-PFC3D numerical model is shown in Figure 2 for the calculation and analysis of the slope stability under the action of tunnel excavation and blasting. The width of the model is 60m, the height is 65m (the height of the accumulation layer is 5m, and the height of the bedrock is 50m), and the thickness is 30m. The specific parameters of the model are shown in Table 1, Table 2 and Table 3.

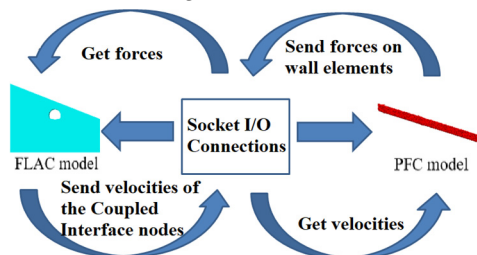


Fig. 1. FLAC3D–PFC3D data transmission diagram

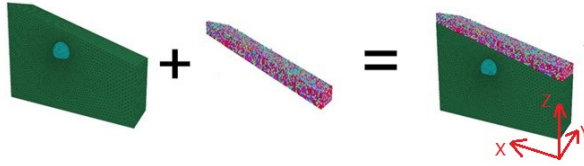


Fig. 2. FLAC3D–PFC3Dcoupled numerical model

Table 1. Macroscopic mechanical parameters of accumulation slope

Material	Gravity γ (kN/m^3)	Modulus of deformation E (GPa)	Poisson ratio μ	Force of cohesion c (kPa)	Angle of internal fric- tion φ ($^{\circ}$)
accumulation	22.4	0.045	0.3	8.5	22.7

Table 2. Microscopic Calculation Parameters of accumulation Slope

Material	Ratio of maximum to minimum particle radius	Density γ ($kg \cdot m^{-3}$)	Friction factor μ	Elastic modulus E/Pa	Parallel bond elastic modu- lus \bar{E} / GPa
accumulation	12	22.4	0.42	4.5e7	0.045

Table 3. Calculation parameters of bedrock

Material	Densi- ty/ ($Kg \cdot m^{-3}$)	Elastic mod- ulus/ GPa	Force of cohe- sion c/MPa	Angle of internal friction $\varphi /$ $^{\circ}$	Uniaxial compres- sion strength of rock/ MPa	Tension strength of rock/ MPa	Friction factor μ
bedrock	1800	3.96	1.63	32	26	0.16	0.3

3.2 Numerical simulation scheme

Under the blasting vibration load, the slope above the tunnel is prone to collapse and landslide. This paper mainly studies the influence of tunnel excavation blasting load parameters on slope stability. By applying the blasting stress wave corresponding to the tunnel blasting load on the blasting hole wall of the working face, the simulation of the tunnel blasting excavation process is realized. According to the site construction scheme, two schemes are set up, among which the first scheme is the working conditions 1, 2 and 3 with the working time of 10ms and the peak value of blasting load of 5MPa, 7.5 MPa and 10MPa respectively, and the second scheme is the working conditions 4, 5 and 6 with the peak value of blasting load of 7.5 MPa and the working time of 20ms, 30ms and 40ms respectively.

In the process of tunnel blasting excavation, the blasting stress wave is usually regarded as a pulse stress wave, and the stress wave propagates from the blast hole wall

to the surrounding area in the form of a spherical wave. In this paper, referring to the blasting seismic wave model established by [13], the blasting stress wave is simplified as a half-sine wave with equal rising and falling time, and its expression is as follows:

$$p(t) = \frac{P_m}{2} (1.0 - \text{COS}(\frac{2\pi}{\Delta T} t)) \quad (1)$$

Among them, P_m is the peak value of blasting load; ΔT is the action time of blasting load stress wave; t is the duration of blasting.

3.3 Boundary condition

In the static boundary condition, the fix constraint in FLAC3D is adopted, and the displacement constraint conditions are imposed on the left and right boundary (x direction), front and back boundary (y direction) and bottom boundary of the model, and the displacement field should be cleared first in the tunnel excavation construction stage. In the dynamic analysis of FLAC3D, the reflection of the reflected wave by the boundary is reduced as much as possible, to reduce the influence of the boundary conditions on the simulation results. In this paper, the viscous boundary condition is adopted, and independent viscous forces are applied to the horizontal and normal directions of the boundary. The formulas for calculating the shear viscous force (f_s) and the normal viscous force (f_n) are as follows:

$$\begin{cases} f_s = -\rho c_s v_s \\ f_n = -\rho c_p v_n \end{cases} \quad (2)$$

Among them, v_s , v_n is the tangential velocity component and normal velocity component on the boundary; ρ is the density of rock mass; c_p and c_s are the velocities of P and S waves.

4 RESULT ANALYSIS

4.1 Analysis of variation law of formation velocity field

According to the coupling calculation of the three-dimensional numerical model of the accumulation slope at the tunnel entrance under different blasting parameters, the nephogram of the vertical velocity field of the stratum with the change of blasting parameters can be obtained, as shown in Figure 3.

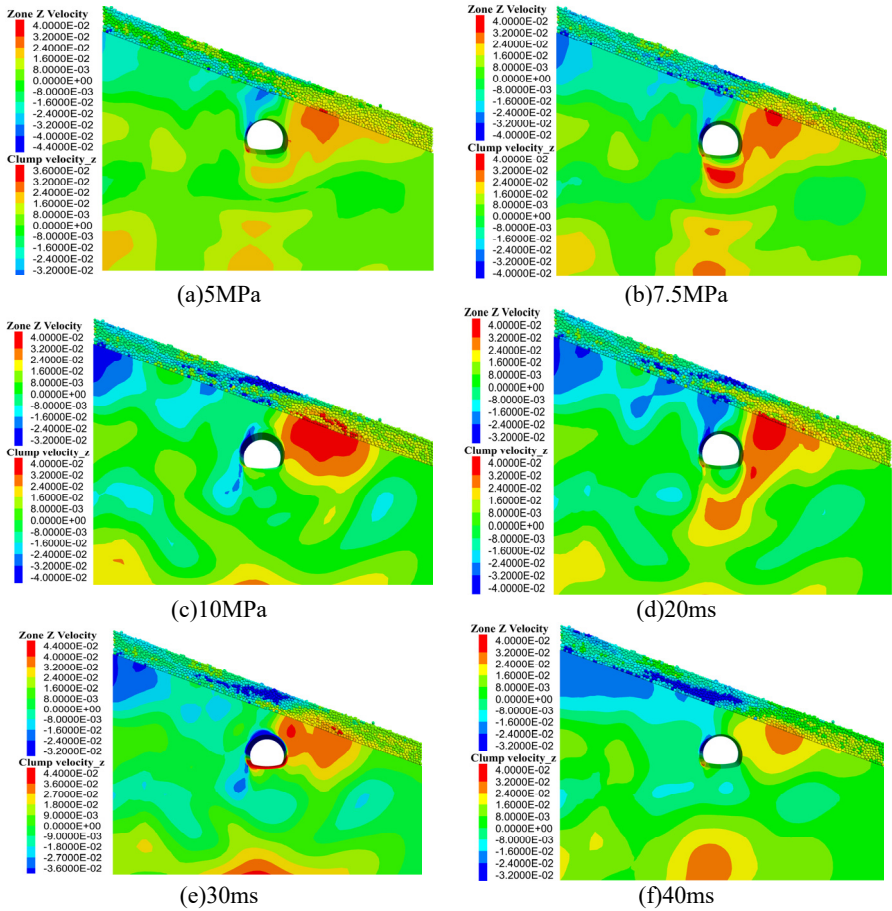


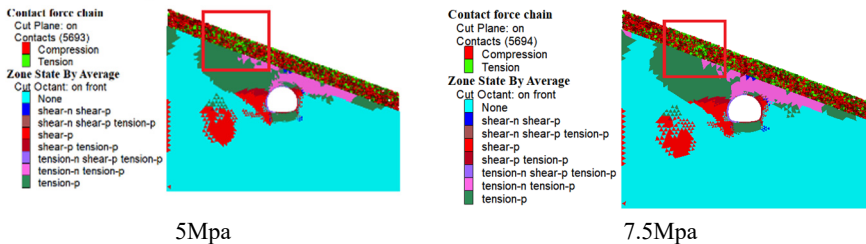
Fig. 3. Vertical velocity distribution nephogram of stratum under different blasting parameters

It can be seen from Fig. 3 that the velocity distribution between the particles in the accumulation layer and the bedrock is continuous, which proves the correctness of the propagation of the explosion stress wave on the coupling interface. According to Fig. 3 (a ~ c), with the increase of the peak value of the blasting load, the blasting stress wave increases as a whole, and its disturbance to the accumulation layer becomes more and more apparent, especially the particles in the accumulation layer above the vault and the right arch shoulder of the tunnel, the range and rate of particle loosening increase significantly, but the velocity direction and location of particles in the two places are different. The particle loosening above the vault mainly occurs in the surface layer of the slope, while the right arch shoulder of the tunnel mainly occurs at the interface, both of which expand to the inside of the slope with the increase of the peak value of load; When the blasting peak load is 10MPa, the surface layer of the accumulation layer above the vault is loosened in a wide range, and the particle velocity exceeds 6cm/s, resulting in poor slope stability. With the increase of blasting time, that

is, the frequency of explosion stress wave decreases. According to Fig. 3 (b, d, e, f), with the increase of blasting time, the range and rate of particle loosening above the tunnel vault increase obviously, and gradually develop towards the inside of the slope and the top of the slope. The overall velocity of particles on the upper part of the slope is more significant, and the maximum velocity on the top of the slope exceeds 4cm/s; The change of particle velocity in the lower part of the slope is small, and the particle stability is good.

4.2 Analysis of Force Chain Distribution in Formation Plastic Zone and Accumulation Zone

Fig. 4 shows the plastic change of surrounding rock and the distribution of particle contact force chain under different working conditions. It can be seen from the figure that under the disturbance of explosion stress wave, the plastic zone of stratum is mainly concentrated in the surrounding rock area around the tunnel, and the plastic zone of the tunnel vault and arch bottom is widely developed. The tensile failure is the main one. There are more tensile force chains in the contact force chains between the particles in the accumulation layer. They are mainly distributed among the particles in the upper part of the slope, especially between the top of the vault and the top of the slope, as shown in Fig. 4 (a, b, c), which indicates that there is a large tensile force between the particles and the contact fracture between the particles increases. When the time of blasting load is 10ms, and the peak value of the blasting load changes, the effect of eccentric pressure on the tunnel is similar. The plastic zone of the tunnel vault roof develops to the interface between the accumulation layer and bedrock, and gradually develops along the interface surface to the top of the slope. Moreover, there is a specific tensile plastic zone at the foot of the slope, and the mutual disturbance between tunnel blasting excavation and the accumulation layer has a strong influence. The plastic zone in the upper part of the slope is much larger than that in the lower part of the stratum, which is because the tunnel is close to the free face of the lower part of the slope. The energy is released quickly, so the plastic zone is small and mainly concentrated at the foot of the slope. However, with the increase of loading time, the area of the plastic zone near the interface between the accumulation layer and stratum increases sharply, which runs through the interface between the accumulation layer and bedrock, and is mainly damaged by tension.



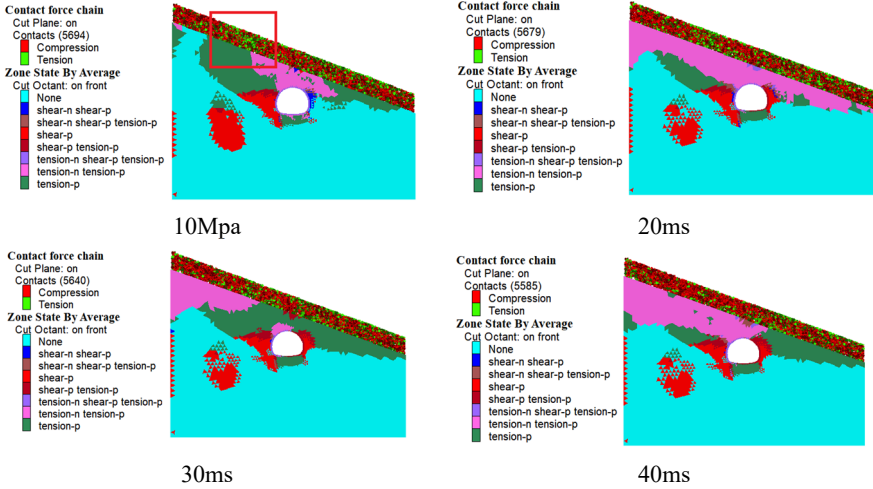


Fig. 4. The distribution of formation plastic zone and accumulation layer force chain

4.3 Slope stability analysis

Under the action of blasting load, the strength reduction method cannot be directly used to solve the slope safety factor because of the embedding of discrete elements in FLAC. When establishing the PFC element model, the friction coefficient, contact bond strength and contact bond tensile strength are important parameters that affect the physical mechanics of the macroscopic model, so the slope safety factor F can be solved by the strength reduction of these three factors. According to the above method, the slope safety factor F is solved by successive reduction. If there is an apparent large-area tension chain at the top of the pile slope or other areas, it is judged as a failure. When the ratio of tensile force chain to bond force chain increases sharply, the safety factor is the reduction factor F for which the model just breaks.

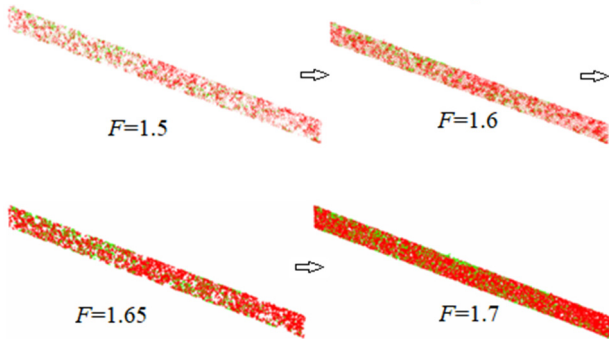


Fig. 5. Force chain distribution diagram of accumulation layer

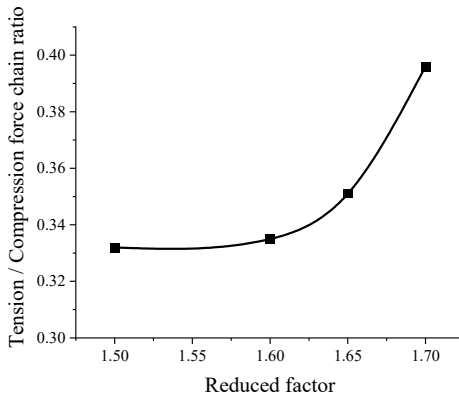


Fig. 6. Stack layer force chain statistical diagram

With the increase of the reduction factor, the accumulation layer is filled with a large number of complicated tension chains, and the inter-granular tension chains in the upper part are increasing and aggregating (see Figure 5), and the accumulation layer tends to be destroyed gradually. According to the ratio of tension force chain to bond force chain (see Figure 6), when the reduction factor F is 1.65, the slope of the curve increases obviously, and it is considered that the accumulation layer is in a critical state of failure at this time; When the reduction factor F is 1.7, the ratio increases rapidly to 0.396, and the slope is considered to be in a state of failure at this time. Hence, the safety factor F of the accumulation slope is 1.65.

5 CONCLUSION

With the research on the slope stability of the accumulation layer at the entrance of the tunnel under the action of tunnel excavation, the main conclusions are as follows:

(1) With the increase of the peak value of blasting load, the sedimentation amount of particles in the accumulation layer increases sharply, the sedimentation tank becomes steeper and deeper, and the change of particle velocity and loose range in the surface layer of the accumulation layer above the tunnel is most apparent, with the maximum particle velocity exceeding 6cm/s; With the increase of load peak from 5MPa to 10MPa, the loose thickness of particles in the vault accumulation layer increased sharply from 1.25 m to 3.75 m, accounting for 3/4 of the accumulation layer thickness. The blasting disturbance of the accumulation layer became more and more apparent.

(2) The plastic zone of the stratum is mainly concentrated in the surrounding rock area around the tunnel. There are many tensile force chains in the contact force chains among the particles in the accumulation layer, which are mainly distributed among the particles in the upper part of the slope, significantly above the vault and at the top of the slope.

(3) The strength of physical and mechanical parameters between particles in the accumulation layer is reduced, and the ratio of tension and bond force chain between particles is taken as the evaluation standard, and the safety factor of slope is solved.

ACKNOWLEDGMENT

This work is supported by the National Natural Science Fund of China (No. 52078090), the general program of Chongqing Natural Science Foundation (No. cstc2020jcyj-msxmX0679), and the Fund of State Key Laboratory of Mountain Bridge and Tunnel Engineering (No. SKLBT-19-006).

REFERENCES

1. Shaorui, S., Penglei, X., Jimin, W., Jihong, W., Wengan, F., & Jin, L., et al. (2014). Strength parameter identification and application of soil-rock mixture for steep-walled talus slopes in southwestern China. *Bulletin of Engineering Geology & the Environment*, 73(1), 123-140.
2. Dong-sheng Xu, Hua-bei Liu, Rui Rui et al. (2019) Cyclic and post cyclic simple shear behavior of binary sand-gravel mixtures with various gravel contents. *Soil Dynamics and Earthquake Engineering*, 123,230-241.
3. Yao, Y., Li, J., Ni, J., Liang, C., & Zhang, A. (2022). Effects of gravel content and shape on shear behaviour of soil-rock mixture: experiment and dem modelling. *Computers and Geotechnics*, 141, 104476-.
4. Li, A., Deng, H., & Zhang, H. (2022). Experimental research on cumulative damage law of microcrystalline limestone under fixed equivalent cyclic blasting load. *Arabian Journal of Geosciences*, 15(2), 1-12.
5. Liu, G., Song, D., & Chen, Z. (2020). Dynamic response characteristics and failure mechanism of coal slopes with weak intercalated layers under blasting loads. *Advances in Civil Engineering*, 2020(9).
6. Chen, M., He, W., Lu, W., Wang, G., & Leng, Z. (2017). Studies on the vibration of tunnel surrounding rock induced by air overpressure. *Zhendong yu Chongji/Journal of Vibration and Shock*, 36(12), 12-17.
7. Wartman, J., Seed, R. B., & Bray, J. D. (2005). Shaking table modeling of seismically induced deformations in slopes. *Journal of geotechnical and geoenvironmental engineering* (5), 131.
8. XIE Haixiang. (2020). Study on vibration characteristics and laws of blasting excavation of mountain tunnel. (Doctoral dissertation, Xi'an University of Technology).
9. Li, Q., Dai, B., Long, L., Zhang, D., & Liang, F. (2022). Response characteristics of slope subjected to blasting: a case study in manaoke open-pit gold mine. *Geotechnical and geological engineering* (8), 40.
10. Yan B., Liu M., Meng Q., Li Y., Deng S., Liu T. (2022) Study on the Vibration Variation of Rock Slope Based on Numerical Simulation and Fitting Analysis. *Applied Sciences* 12(9), 4028.
11. Azizabadi, H., Mansouri, H., & Fouche, O. (2014). Coupling of two methods, waveform superposition and numerical, to model blast vibration effect on slope stability in jointed rock masses. *Computers & Geotechnics*, 61(sep.), 42-49.

12. Huang F, Wang Y, Wen Y B, et al. (2019). The deformation and failure analysis of rock mass around tunnel by coupling finite difference method and discrete element method[J]. Indian Geotechnical Journal, 49(4), 421-436.
13. LONG Yuan, FENG Changgen, XU Qunjun, et al. (2000). Study on propagation characteristics of blasting seismic waves in a rock medium and numerical calculation. Engineering Blasting, 6(3), 1-7.

Open Access This chapter is licensed under the terms of the Creative Commons Attribution-NonCommercial 4.0 International License (<http://creativecommons.org/licenses/by-nc/4.0/>), which permits any noncommercial use, sharing, adaptation, distribution and reproduction in any medium or format, as long as you give appropriate credit to the original author(s) and the source, provide a link to the Creative Commons license and indicate if changes were made.

The images or other third party material in this chapter are included in the chapter's Creative Commons license, unless indicated otherwise in a credit line to the material. If material is not included in the chapter's Creative Commons license and your intended use is not permitted by statutory regulation or exceeds the permitted use, you will need to obtain permission directly from the copyright holder.

